Journal of Thermal Biology 83 (2019) 103–111

Contents lists available at ScienceDirect

Journal of Thermal Biology

journal homepage: www.elsevier.com/locate/jtherbio

The thermal performance of biological tissue under moxibustion therapy

Chao Sun[a], Ying Li[a], Jiujie Kuang[a,*], Ximei Liang[a], Jiangtao Wu[a], Changchun Ji[b]

[a] Key Laboratory of Thermo-Fluid Science and Engineering of MOE, Xi'an Jiaotong University, Xi'an, 710049, China
[b] Bioinspired Engineering and Biomechanics Center (BEBC), Xi'an Jiaotong University, Xi'an, 710049, China

ARTICLE INFO

Keywords:
moxibustion therapy
Ash cleaning
Distance adjustment
Computational modeling
Thermal performance

ABSTRACT

An understanding of the thermal performance of biological tissue under moxibustion with ash cleaning and distance adjustment (ACDA) is helpful for the optimization and standardization of moxibustion clinical treatment. This study compared surface temperature distribution of burning moxa stick with and without ash cleaning. The experimental of moxibustion treatment on in-vitro tissue and human abdomen were conducted and corresponding numerical models were developed. The effect of ACDA on thermal performance of biological tissue under moxibustion therapy were analyzed. The results show that the surface temperature of burning moxa stick with ash cleaning maintained at a higher range compared to that without ash cleaning. During moxibustion with ACDA process in in-vitro tissue experiment, the temperature increase (ΔT) at skin surface almost fluctuated in the same temperature range, and the ΔT in subcutaneous tissue ($>$ 11 mm) kept increasing. Relatively, these ΔT under moxibustion treatment without ACDA showed different trends and these values were all much smaller than those with ACDA. In addition, the position of maximum temperature of tissue under moxibustion with and without ACDA was fixed on treatment acupoint and moved away from treatment acupoint, respectively. Besides, the surface temperature of human abdomen tissue under moxibustion treatment with ACDA can be maintained at 46 °C–50 °C for a longer time compared to that under moxbustion without ACDA. In conclusion, moxibustion with ACDA can create a larger and more durable thermal effect on biological tissue. The results also suggest that ACDA may be helpful to improve moxibustion therapy efficacy in clinic treatments.

1. Introduction

Moxibustion therapy is one of the most widely used thermal therapies in traditional Chinese medicine, which delivers heat stimulation to specific areas of body such as meridian points (World Health Organization Western Pacific Region, 2007; Tang et al., 2008). In recent years, moxibustion therapy is drawing more and more attention as its effectiveness for various diseases has been shown in clinical trials, especially in the treatment of fetus breech presentation, and ulcerative colitis (Wheeler et al., 2009; Xu and Yang, 2009; Lee et al., 2010; Kim et al., 2011). As a commonly used method of moxibustion, gentle moxibustion performs by holding a burning moxa stick (Mugwort; Artemisia vulgaris) directly over the skin surface at a certain distance, keeping the spot warm and making it reddened but not burnt (World Health Organization Western Pacific Region, 2007).

With the gradual promotion of moxibustion therapy applications, studies on its underlying mechanisms have been performed. Heat stimulation, optical radiation and some pharmacological effects from moxa are believed to contribute to the therapeutic effect of moxibustion. Among them, heat stimulation plays a major role by promoting trichangiectasis, strengthening metabolism, accelerating absorption and so on (Sakagami et al., 2005; Petrofsky and Laymon, 2009; Chiu, 2013). As shown in Fig. 1, the heat generated by burning moxa stick is transferred from skin surface to inside tissues. This heat transfer process involves heat conduction, heat convection and heat radiation. Some studies have demonstrated that a certain temperature value may exist to obtain desired therapeutic effect of moxibustion (Chen, 2011). For example, the cutaneous thermoreceptors of TRPV1 and TRPV2 can be activated when the temperature reach above 43 °C and 52 °C, respectively, during moxibustion (Jiang et al., 2016). The study by Adriaensen et al. (1983) showed that the temperature range of 44.5 °C–46.5 °C can activate A-fiber mechano-heat-sensitive nociceptors in human skin. Therefore, it is important to keep the effective temperature range of biological tissue during moxibustion in clinic treatments to achieve a better therapeutic effect.

The temperature of biological tissue during moxibustion can be effected by treatment duration, treatment distance, ash deposition and so on. In our previous study (Li et al., 2018). The temperature of biological tissue decreased quickly due to the ash deposition on moxa stick and the increase of treatment distance between the burning moxa stick and

* Corresponding author.
E-mail address: jjkuang@mail.xjtu.edu.cn (J. Kuang).

https://doi.org/10.1016/j.jtherbio.2019.05.018
Received 26 July 2018; Received in revised form 15 May 2019; Accepted 19 May 2019
Available online 23 May 2019

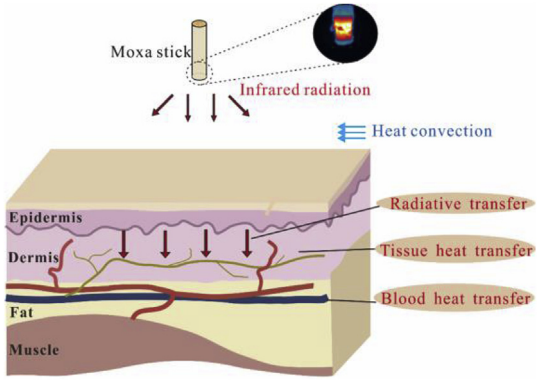

Fig. 1. Schematic of heat transfer process during gentle moxibustion.

tissue during gentle moxibustion. Thus, the therapeutic effect will be weaken owing to the decrease of effective heat stimulation from burning moxa stick. In clinic treatments, clearing the moxa ash and adjusting the distance between the burning moxa stick and skin timely can strengthen the heat stimulation of moxibustion effectively (Wang and Xu, 2010). Our study (Sun et al., 2017) showed that ash cleaning could effectively extend the high temperature duration of moxa sticks and accelerate the burning velocity. Zhou et al. (2014) observed that the temperature of testing area at a 2 cm distance away from the burning surface of moxa stick can maintained at about 47 °C–48 °C when the burnt ashes were removed every 2 min.

Some experiments and models have investigated the detailed temperature distribution of biological tissues during moxibustion. Nakamura et al. (2011) focused attention on temperature distribution of a phantom model and human body during moxibustion and measured temperatures by Magnetic Resonance Imaging (MRI) equipment. Ying et al. (2015) investigated the skin temperature distribution of Zusanli acupuncture point area among the treatments of mild moxibustion, moxibustion with monkshood and moxibustion with ginger. They found that different moxibustion methods could result in different temperature distributions. Myoung et al. (Myoung and Lee, 2014) compared the temperature differences in rabbit tissue between the influence of moxibustion and an electrical thermal stimulation system using optical fiber temperature sensor. Jeon et al. (Jeon and Choi, 2010) solved the problem of unsteady convective heat transfer coupled with conductive heat transfer in indirect moxibustion to get the body's temperature history based on ANSYS-Fluent, and they revealed the interaction of indirect moxibustion with the body and surrounding fluid. Huang et al. (Huang and Sheu, 2013) established a three-dimensional human calf model containing some superficial vessels to get the temperature distribution beneath the skin surface during moxibustion therapy, and they revealed the effect of moxibustion on the blood flow in vessels and vice versa based on the model. However, the thermal performance of moxibustion with ACDA has been rarely reported so far. To improve the effectiveness of moxibustion, it is imperative to obtain the spatial and temporal temperature distribution in tissues and study the effect of ACDA on thermal performance of moxibustion therapy. In addition, burning moxa stick produces heat stimulation and unique therapeutic effects during moxibustion (Chiu, 2013). The research on temperature distribution of burning moxa sticks is primary for better understanding of thermal performance of moxibustion therapy.

In the present paper, the thermal performance of burning moxa stick with and without ash cleaning were studied using an infrared camera, and the temperature distributions in in-vitro porcine abdominal tissue during moxibustion with and without ACDA were compared experimentally. Subsequently, models for burning moxa stick with and without ash cleaning, and moxibustion in the in-vitro tissue with and without ACDA were developed to analyze the detailed heat transfer process of burning moxa stick and temperature distribution of tissue respectively. And the model predictions were consistent well with experimental results. Meanwhile, in order to study the effect of ACDA on moxibustion in human, the surface temperature distributions of human abdominal tissue during moxibustion with and without ACDA were recorded using an infrared camera. And the temperature distributions of human abdominal subcutaneous tissue were compared by models which were built based on corresponding in-vitro tissue models respectively with a well consistent tissue surface temperature between experimental results and simulative predictions.

2. Experimental details

2.1. Moxa stick burning measurement

Pure moxa sticks, 1.8 cm in diameter (d), 20 cm in length and 20 g ± 0.2 g in weight, were used in the experiment. Moxa sticks suspended vertically were ignited. For the burning moxa stick without ash cleaning, the ash deposited on burning surface of moxa stick was not removed. While for the case with ash cleaning, the ash was cleaned every 4 min. The temperature history of their burning lower surface and side surface were recorded by a calibrated infrared camera (FLIR T420). The sensitivity, accuracy and resolution for the employed camera are 0.045 K, ± 2 K and 320 × 240 pixels, respectively.

2.2. Moxibustion in the in-vitro tissue measurement

In clinical treatment, in order to keep effective heat stimulation, clinicians often remove the ash and adjust the distance between burning moxa stick and skin timely instead of leaving the burning moxa stick alone during moxibustion. In this part, the temperature distributions of in-vitro tissue between moxibustion without ACDA and moxibustion with ACDA were compared to study the effect of ash cleaning and distance adjustment on thermal performance of moxibustion therapy, and the two moxibustion operations were denoted as Case I and Case II for convenience, as shown in Table 1. Fresh in-vitro porcine abdominal tissues which closely resemble human tissue with respect to histological, physiological, and immunological properties were used as experimental samples (Vardaxis et al., 1997). The tissues were bought from a butcher shop within 6 h post-sacrifice and were cut into two rectangle-shaped pieces with roughly equal structure for experiments. The schematic diagram of the moxibustion experimental setup is shown in Fig. 2(a). The temperature in tissue surface were monitored with the calibrated infrared camera (FLIR T420). Temperature histories inside tissue were recorded with T type thermocouples which were introduced into the tissue via stainless steel needles. As shown in Fig. 2(b),

Table 1
Moxibustion with different operations for ash deposition and distance adjustment.

Case	Ash cleaning	D_1 (Initial value = 3 cm)	D_2
I	No	Increased with the upward burning of moxa stick	Fixed
II	Yes	Adjusted to 3 cm after every ash cleaning	Decreased due to the adjustment
III	Yes	Increased with the upward burning of moxa stick	Fixed

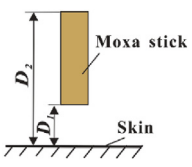

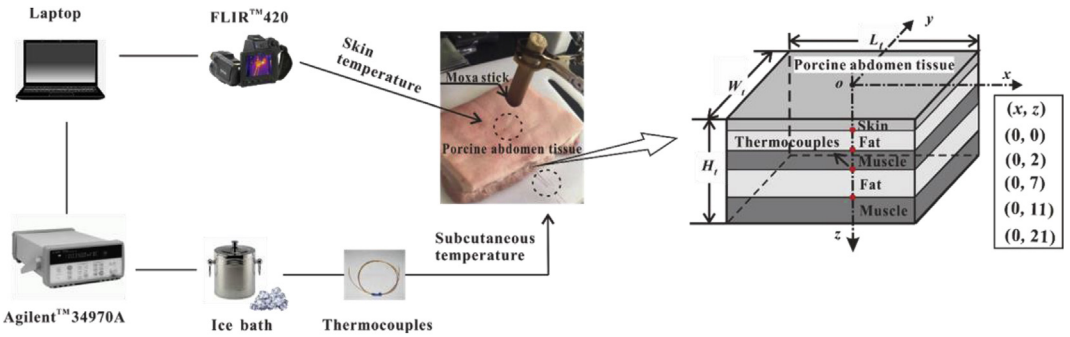

(a) (b)

Fig. 2. Schematic diagram of the moxibustion experiment: (a) experimental setup; (b) Thermocouples distribution in in-vitro tissue (Sun et al., 2017).

thermocouples were positioned in every layer interface of porcine abdominal tissue along the central axis and the cold junctions of thermocouples were embedded into an ice bath. Temperature data from thermocouples were recorded every 5 s by a data acquisition unit (Agilent™, 34970A). The thermocouples were calibrated in an appropriate temperature range before moxibustion experiments.

The moxa stick were fixed above the in-vitro porcine tissue vertically and the distance between the moxa stick and the sample surface was 3 cm (D), which is a comfortable distance in clinical moxibustion treatment (Liu et al., 2017). For Case I, the burning moxa stick was leaved alone during moxibustion treatment. While for Case II, the moxa stick was moved away slightly every 4 min to clean ash and the distance between the lower surface of moxa stick and the upper surface of tissue was adjusted to 3 cm after every ash cleaning operation. The whole experimental duration was 40 min including 5 min of initial process, 20 min of stimulation process and 15 min of natural cooling process. The temperature changes during the whole experiment were recorded. All moxibustion experiments were performed under quiet environment and the room temperature was maintained at 22 °C.

2.3. Moxibustion in human abdomen measurement

To study the effect of ACDA on the thermal performance of moxibustion in human detailedly, based on the experiment of moxibustion in the in-vitro tissue measurement, the temperature distribution of human's abdominal skin during moxibustion with ash cleaning but no distance adjustment was investigated additionally. And the additional case was denoted as Case III for convenience, as show in Table 1. In this experiment, Zhongwan (CV 12) acupoint was chosen as the moxibustion treatment point. Based on the Science of Acupuncture and Moxibustion, Zhongwan acupoint is located at the middle of the stomach at the level of the pylorus, between the solar plexus and umbilical ring (Jun et al., 2007), which is the specific treatment point for improving immunity and gastrointestinal function. The moxa stick were fixed above the Zhongwan acupoint vertically and the initial distance between the moxa stick and skin was 3 cm. The operations for Case I and Case II were the same as those in moxibustion in the in-vitro tissue measurement. For Case III, the moxa stick was moved away slightly every 4 min to clean ash and then it was moved back directly with no distance adjustment. The whole experimental duration were all the same as those in moxibustion in the in-vitro tissue measurement. Changes of the skin surface temperature during the whole experiment were recorded with the infrared camera. This experiment performed on five volunteers repeatedly who were recruited from Xi'an Jiaotong University. All participants received the appropriate information about the study characteristics and signed an informed consent before their inclusion in the study. The protocol of this experiment was approved by the Ethics Committee of the Xi'an Jiaotong University.

3. Numerical modeling

3.1. Model assumptions

The moxibustion model includes moxa stick burning model and tissue bio-heat transfer model. The moxa stick burning model and in-vitro porcine tissue model have been established and described in detail previously (Sun et al., 2017; Li et al., 2018). In this study, the moxibustion model for human abdominal tissue was developed based on the in-vitro moxibustion model to predict outcome in clinic moxibustion treatment.

As described in our previous study (Li et al., 2018), the geometries of moxa stick and tissue were assumed to be symmetric to the axis, and the model was simplified to be a two-dimensional axisymmetric shape in cylindrical coordinates, as shown in Fig. 3.

The moxa stick model with 9 mm in radius (R_m) and 80 mm in length (H_m) is divided into five parts from bottom to top along the axis to simulate the different temperature areas during moxa stick burning. They are Ω_1, Ω_2, Ω_3, Ω_4, and Ω_5 which represent unburnt area, pyrolysis area, high temperature burning area, lower temperature burning area, and ash content area, respectively, as shown in Fig. 3. The height of each area varies with time during burning, so we can assume that each area moves up with different velocities. The velocities v_i of different areas in burning moxa stick with and without ash cleaning were obtained based on experimental observation respectively, as listed in Table 2. The geometry of in-vitro tissue model was calculated based on the same height and volume as each layer of the in-vitro porcine abdominal tissue sample used in experiments and the thickness of each layer was shown in Table 3. The tissue is assumed to be homogenous and its thermophysical properties are independent of temperature. The parameters of each layer are shown in Table 3 (Henriques and Moritz,

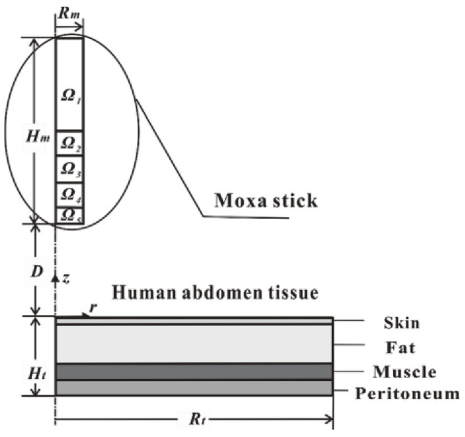

Fig. 3. Geometries of the moxibustion model.

Table 2
Movement speeds of different areas in burning moxa stick.

	Ω_i	H_{i0} (mm)	v_i (10^{-5}m s^{-1})	t (s)					
				0–100	100–180	180–300	300–800	800–1000	1000–1200
Without ash cleaning	Ω_1	68.7	v_1	3.08	3.08	3.08	2.85	2.66	2.66
	Ω_2	5	v_2	2.475	2.475	2.475	2.475	2.4	2.4
	Ω_3	3.3	v_3	0	1.33	1.33	2.17	2.17	2.17
	Ω_4	3	v_4	0	1.014	1.014	1.014	1.014	1.875
	Ω_5	0	v_5	0	0	0	0.678	0.678	0.678
With ash cleaning	Ω_1	68.7	v_1	3.08	3.08	3.08	2.85	2.66	2.66
	Ω_2	5	v_2	2.475	2.475	2.475	2.475	2.4	2.4
	Ω_3	3.3	v_3	0	1.33	1.33	2.17	2.17	2.17
	Ω_4	3	v_4	0	2.35 × 10-8t2				
	Ω_5	0	v_5	$v5 = 0$, while 0 [a] t2 ≤ 165; $v5 = 1.42 \times 10$-2t2, while 165 ≤ t2 ≤ 180[a]					

[a] $t_1 = t/180$; $t_2 = t - [t_1]\cdot 180$, $[t_1]$ represents the biggest integer which is not more than t_1.

Table 3
Thermal properties of in-vitro porcine abdominal tissue.

Tissue	h_t (mm)	k_t (W/m·K)	c_t (J/kg·K)	ρ_t (kg/m^3)
Skin	2	0.205 ($0 \geq z > -0.1$) 0.370 ($-0.1 \geq z \geq -2$)	3250	930
Fat	5	0.233	1806	1102
Muscle	4	0.459	2624	1178
Fat	3	0.233	1806	1102
Muscle	7	0.340	2624	1178
Fat	4	0.346	2215	1140

1947; Erdmann and Gos, 1990; El-Brawany et al., 2009; Choi et al., 2013).

The human abdominal tissue can be divided into about four layers, including skin, fat, muscle and peritoneum (Ahuja et al., 1978; Werner and Buse, 1988; Wilson et al., 1988; Torvi and Dale, 1994; Cheng and Herman, 2011). The tissue is assumed to be homogenous and its thermophysical properties are independent of temperature. The parameters of each layer used in the in-vivo tissue model are listed in Table 4.

3.2. Governing equations

The origin of the coordinate system is located at the center of the upper surface of the tissue as shown in Fig. 3. Based on the above model assumptions, the heat transfer process for burning moxa stick was governed by the Fourier's partial differential heat equation as follows:

$$\rho_m c_m \frac{\partial T}{\partial t} = \nabla\cdot(k_m \nabla T) + Q_i \quad (1)$$

where ρ_m, c_m and k_m are density (kg m^{-3}), specific heat (J kg^{-1} K^{-1}), and thermal conductivity of moxa stick (W m^{-1} K^{-1}), respectively. Q_i is the heat source existed in moxa stick and it is described in detail next.

The thermal performance of tissue beneath the skin obeys the Pennes bio-heat equation (Pennes, 1984).

$$\rho_t c_t \frac{\partial T}{\partial t} = \nabla\cdot(k_t \nabla T) + \rho_b c_b w_b (T_a - T) + Q_{met} + Q_s \quad (2)$$

where ρ_t, c_t and k_t are density (kg m^{-3}), specific heat (J kg^{-1} K^{-1}) and thermal conductivity of tissue (W m^{-1} K^{-1}), respectively. ρ_b and c_b are the density (kg m^{-3}) and the specific heat of blood (J kg^{-1} K^{-1}), respectively. w_b is the blood perfusion rate (s^{-1}), Q_{met} is the volumetric metabolic heat (W m^{-3}), and Q_s is the heat source term (W m^{-3}).

Table 4
Thermal properties of human abdominal tissue.

Layer	Tissue	D_i (mm)	k_t (W m^{-1} K^{-1})	c_t (J kg^{-1} K^{-1})	ρ_t (kg m^{-3})	w_b (s^{-1})	Q_{met} (W m^{-3})
1	Skin	2	0.445	3300	1200	0.00064	368.1
2	Subcutaneous fat	15	0.185	2674	1000	0.00008	368.3
3	Muscle	5	0.51	3800	1085	0.0027	684.2
4	Peritoneum	5	0.185	2674	1000	0	368.3

No blood perfusion and metabolic exist in in-vitro tissue, so we treated w_b and Q_{met} as zero. With regard to in-vivo tissue, the blood perfusion and metabolic activity exist in every layer of the tissue, and the relevant thermophysical properties of each layer are listed in Table 4 (Ahuja et al., 1978; Werner and Buse, 1988; Wilson et al., 1988; Torvi and Dale, 1994; Cheng and Herman, 2011).

The top surface of moxa stick and the lower surface of tissue are considered as thermal insulating boundary conditions during the whole simulation process. And natural convection occurs in other surfaces of moxa stick and tissue. Besides, surface to surface radiation is performed between the outside surface of burning moxa stick and the top surface of tissue during moxibustion. Considering that for moxibustion with ACDA, the moxa stick was moved away to clean the ash for 15 s every 4 min and the distance between the moxa stick and skin was adjusted to 3 cm after every ash cleaning operation during moxibustion, the emissivity of tissue and moxa stick were set as zero in a time interval of 15 s during every ash cleaning operation and then the distance was also adjusted to 3 cm. Initial temperatures of moxa stick, tissue and surroundings are set in consistent with experimental data.

3.3. Heat source

The heat source term Q_i in (1) represents heat production of moxa stick. According to the regionalization of burning moxa stick, Q_i of each area for burning moxa stick with and without ash cleaning are fitted by polynomial based on experiment results, as listed in Table 5.

The heat source term Q_s in (2) includes Q_w and Q_r, which were equivalent to water evaporation and radiation attenuation in in-vitro tissue respectively. And for in-vivo tissue, no water evaporation occurs, so Q_s equals to Q_w. The Q_w and Q_r, in this study were set at the same values as in our previous paper (Li et al., 2018).

3.4. Numerical procedure

The whole simulation process including geometric modeling, mesh generation, calculation and so on were all performed in COMSOL Multiphysics software based on finite element method (FEM). The thermal equations coupled with radiation equations were solved transiently. The simulation results with different fine degree of mesh mapping for multilayered tissue and moxa stick were compared and the most suitable meshes which was sufficient to obtain grid independent results were determined finally. The choice of time steps were determined by taking into account computational convergence and efficiency. 0.1 s and 0.3 s were chosen for the simulation process: moxibustion process (20 min) and natural cooling process (15 min),

Table 5
Fitted equations of heat source of different areas in moxa stick.

Ω_i	Q_i (W m^{-3})	Without ash cleaning	With ash cleaning
Ω_1	Q_1	$Q_1 = 1.1705 \times 10^7 - 1.0344 \times 10^4 t - 1.0568 \times 10^2 t^2 + 3.466 \times 10^{-1} t^3 - 4.2362 \times 10^{-4} t^4 + 2.3196 \times 10^{-7} t^5 - 4.7556 \times 10^{-11} t^6$	$Q_1 = 9.5981 \times 10^6 - 8.4821 \times 10^3 t - 8.6658 \times 10 t^2 + 2.8421 \times 10^{-1} t^3 - 3.4737 \times 10^{-4} t^4 + 1.9021 \times 10^{-7} t^5 - 3.8996 \times 10^{-11} t^6$
Ω_2	Q_2	$Q_2 = 3.8358 \times 10^7 - 1.3174 \times 10^5 t - 5.3817 \times 10^2 t^2 + 1.7222 t^3 - 2.8453 \times 10^{-3} t^4 + 2.1494 \times 10^{-6} t^5 - 5.9522 \times 10^{-10} t^6$	$Q_2 = 3.1454 \times 10^7 - 1.0803 \times 10^5 t - 4.4130 \times 10^2 t^2 + 1.4122 t^3 - 2.3331 \times 10^{-3} t^4 + 1.7625 \times 10^{-6} t^5 - 4.8808 \times 10^{-10} t^6$
Ω_3	Q_3	$Q_3 = (1.2065 \times 10^7 - 9.2794 \times 10^4 t + 2.1774 \times 10^2 t^2 - 1.012 \times 10^{-1} t^3)/(1 - 6.573 \times 10^{-3} t + 9.853 \times 10^{-6} t^2 + 1.614 \times 10^{-8} t^3)$	$Q_3 = \begin{cases} 1.1188 \times 10^7, 0 \le t_2 \le 40^a \\ 1.3551 \times 10^7 - 4.2178 \times 10^4 t_2, 40 \le t_2 \le 165 \\ 1.3402 \times 10^7 - 4.1714 \times 10^4 t_2, 165 \le t_2 \le 180 \end{cases}$
Ω_4	Q_4	$Q_4 = 0.8958/(6.536 \times 10^{-8} + 5.219 \times 10^{-10} t - 7.085 \times 10^{-11} t^2 + 2.081 \times 10^{-12} t^3 - 3.813 \times 10^{-14} t^4 + 1.904 \times 10^{-16} t^5)$	$Q_4 = \begin{cases} 1.3892 \times 10^7, 0 \le t_2 \le 30 \\ 2.3648 \times 10^7 - 1.9705 \times 10^5 t_2, 30 \le t_2 \le 120 \\ 0, 120 \le t_2 \le 180 \end{cases}$
Ω_5	Q_5	0	0

[a] $t_1 = t/180$; $t_2 = t - [t_1] \cdot 180$, $[t_1]$ represents the biggest integer which is no more than t_1.

respectively.

4. Results and discussion

4.1. Moxa stick burning characteristics

In order to acquire burning characteristics of the moxa stick, temperature distributions on its lower surface and side surface were recorded with an infrared camera during burning. The infrared images of the side surface of the burning moxa stick without ash cleaning at $t = 20$ min are shown in Fig. 4(ii). It can be seen that five clear areas were distributed in the side surface of burning moxa stick: ash content area, high temperature burning area, low temperature burning area, pyrolysis area and unburnt area (Xia, 2008; Li et al., 2018). Every area moved with time during buring of moxa stick. The velocities (v_i), as listed in Table 1, were calculated by measuring the movement of each areas based on infrared images of burning moxa sticks. Fig. 4(i) shows the infrared images of the side surface of the burning moxa stick at different time. (a) ~ (c) and (d) ~ (f) in Fig. 4(i) represent burning without and with ash cleaning respectively. From (a) ~ (c) in Fig. 4(i) it can be observed that burning areas moved up with time and ash deposited on surfaces of burning moxa stick, and obvious ash depositions appeared at $t = 20$ min. Compared (b) and (e) in Fig. 4(i), ash deposition on surfaces could be removed away effectively with the operation of ash cleaning. (f) in Fig. 4(i) depicts that after four times of ash cleaning, the lower surface of moxa stick moved up for a large distance from its original position, which indicates that the burning velocity was distinctly accelerated by ash cleaning. A possible explanation for this result is that the oxygen was more sufficient after ash cleaning. Besides, the infrared images of the burning areas in moxa sticks became highlight after every ash cleaning, which demonstrated that the operation of ash cleaning could lead to a sharp increase of temperature in burning moxa sticks. Therefore, the high temperature area on the surface of burning moxa stick could be kept in a lager area during the whole burning process, whereas lower temperature area of burning moxa stick without ash cleaning appeared in the bottom surface gradually with the ash deposition.

In clinic treatments, the lower surface of burning moxa stick is usually suspended over the patients' skin and produces the heat stimulation to cure disease. The average temperatures on lower surface of the burning moxa sticks with and without ash cleaning are compared in Fig. 5. The solid lines and dotted lines represent the experimental results and simulated predictions respectively, and the black and red lines represent the average temperatures of burning moxa stick without and with ash cleaning respectively. It can be seen that the maximum average temperatures under two cases were the same in general, which demonstrates that the maximum temperature of moxa stick during sufficient burning may be a constant value (about 510 °C). After a 2-min increase at the beginning, the average temperature on the lower surface of the burning moxa stick without ash cleaning kept decreasing to about 150 °C due to the ash deposition. Whereas, the average temperature of burning moxa stick with ash cleaning increased immediately after the ash was removed and then decreased with time showing a zigzag fluctuation in one higher temperature range (about 350 °C–510 °C) during the whole burning process. These results suggest that the operation of ash cleaning can accelerate the burning of moxa sticks and makes them into continuous heat sources with higher temperature relatively. Besides, Fig. 5 also indicates that the simulated predictions agreed well with the experimental results in general. Therefore, the moxa stick burning models with and without ash cleaning are reliable

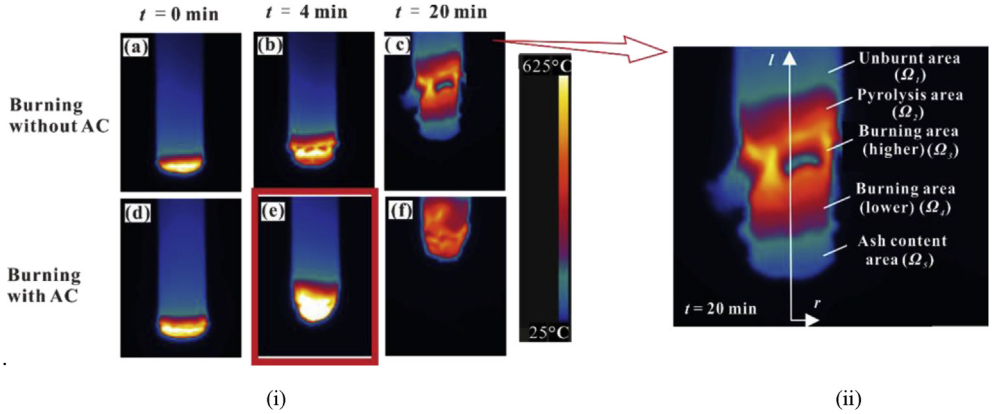

Fig. 4. Infrared image of the burning moxa stick on the side surface: (i) with ash cleaning (AC) and without ash cleaning at different time; (ii) without ash cleaning at t = 20 min.

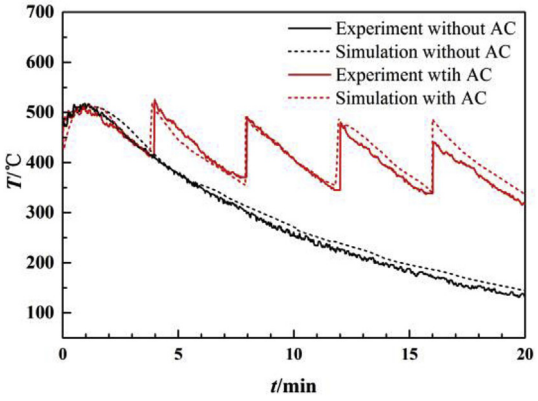

Fig. 5. Comparison of average temperatures on the lower surface of the burning moxa stick with ash cleaning (AC) and without ash cleaning.

to reveal the burning disciplinarian of moxa sticks. And these models provide the foundation for simulation studies on thermal performance of moxibustion in biological tissue.

4.2. Thermal performance of moxibustion in the in-vitro tissue

The thermal performance of the in-vitro tissue between moxibustion without ACDA (Case I) and moxibustion with ACDA (Case II) were compared experimentally and numerically as a foundation to study the effect of ACDA on moxibustion therapy. As shown in Fig. 2(b), the monitoring points were arranged along the central axis of tissue with 0 mm, 2 mm, 7 mm, 11 mm and 21 mm away from the surface. Three processes were included in moxibustion experiments: initial process, moxibustion process and natural cooling process.

Fig. 6 shows the transient temperature increases (ΔT) of monitoring points in porcine tissue in Case I. The solid lines represent experimental results. The ΔT were attained by subtracting initial temperatures from transient temperatures. During moxibustion without ACDA, the ΔT of tissue surface reached maximum value (about 20 ˚C) in about 3 min and then kept decreasing to only nearly 7 ˚C at the end of moxibustion. In natural cooling process, all ΔT declined to relative stable values and remained greater than zero, which indicated that the thermal effect of moxibustion on in-vitro tissue continued after the moxibustion treatment. According to the moxibustion model in our previous study (Li et al., 2018), a numerical model of moxibustion without ACDA in in-vitro tissue was established. The dash lines in Fig. 6 represent the simulation predictions. It can be seen that the predictions of the model agreed with experimental results on the whole.

Fig. 7 depicts the temperature increases (ΔT) of monitoring points in porcine tissue in Case II. The solid lines represent the experimental

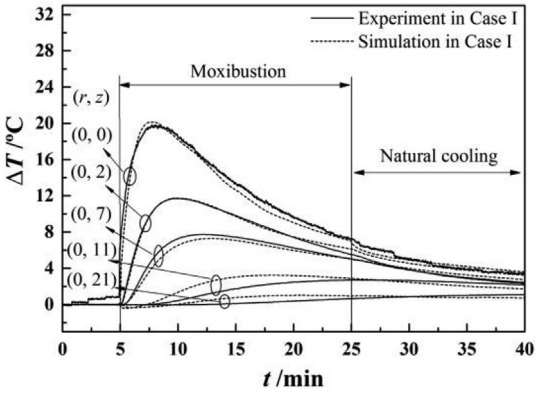

Fig. 6. Transient temperature increases at monitoring points in in-vitro tissue during moxibustion without ACDA (Case I) in experiment and simulation.

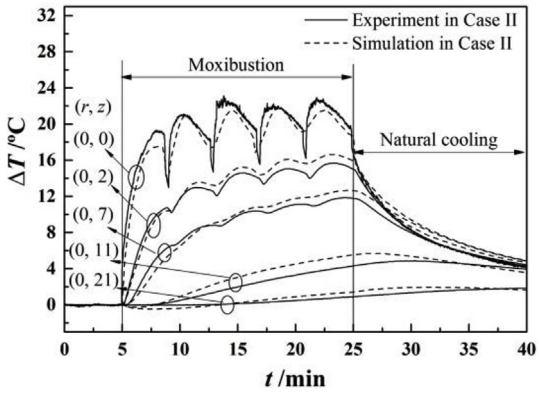

Fig. 7. Transient temperature increases at monitoring points in in-vitro tissue during moxibustion with ACDA (Case II) in experiment and simulation.

results. The ΔT of tissue surface reached maximum value (about 23 ˚C) and kept constant after two times of ash cleaning operation. Comparing the corresponding curves of (0, 2), (0, 7), (0, 11) between Figs. 6 and 7, the ΔT in subcutaneous tissue in Case II kept increasing and were all much higher than those in Case I. The results are reasonable because the ash deposition on the moxa stick surface impeded the energy transfer from burning moxa sticks to tissue and isolated the burning moxa sticks from oxygen, and the increase of distance in Case I reduced the radiation energy which would be absorbed by tissue. After natural cooling, final temperatures of all monitoring points in Case II were higher than those in Case I which demonstrated that ACDA can produce higher final temperatures inside tissue leading to continuous thermal effect. Meanwhile, a numerical model for moxibustion with ACDA in in-vitro tissue was built to predict the detailed temperature distribution of tissue. The dash lines in Fig. 7 represent the simulation predictions, which were consistent with the experimental results generally.

As mentioned above, all predictions of the moxibustion with and without ACDA models fitted the experimental results well, which verified that the two models are reliable to predict the temperature distribution details of in-vitro tissue under moxibustion treatment. The two models also provide the foundation for simulation studies on thermal performance of moxibustion in the in-vivo tissue. The comparison of simulated temperature distributions of in-vitro tissue in Case I and Case II is shown in Fig. 8. Fig. 8(a) presents the 3-D graph of temperature distribution of in-vitro tissue under moxibustion treatment at $t = 15$ min. Relatively, moxibustion with ACDA had an obvious larger domain of thermal effect in the tissue. Fig. 8(b) and (c) depict the simulated temperature distribution in in-vitro porcine abdominal tissue along radius at different depth under moxibustion treatment at $t = 15$ min and $t = 25$ min respectively. As show in Fig. 8(b), at $t = 15$ min, the temperature curves at $z = 0$ mm and $z = 7$ mm in Case II were higher than corresponding temperature curves in Case I when $r < 3$ cm, which indicated that ACDA can induce a higher temperature of thermal effect domain ($0 < z < 7$ mm, $0 < r < 3$ cm). Besides, comparing Fig. 8(b) and (c), the corresponding radius (r) of intersection points between two temperature curves at the same depth under two different cases extended over time, which demonstrated that moxibustion with ACDA can produce a lager thermal effect domain and the differences between the two thermal effect domains expanded along radius and depth with time.

As shown in Fig. 8(b) and (c), the corresponding position of maximum temperature at skin surface in Case I was at center of treatment site at $t = 15$ min, and this position moved to the site at about $r = 1.5\,d$ at $t = 25$ min. The movement of the position of maximum surface temperature can be explained by the variation of radiation range of burning moxa stick, as shown in Fig. 9. During moxa stick burning without ACDA, the ash content formed at the bottom of moxa stick was accumulated to a thick layer with time, and the high

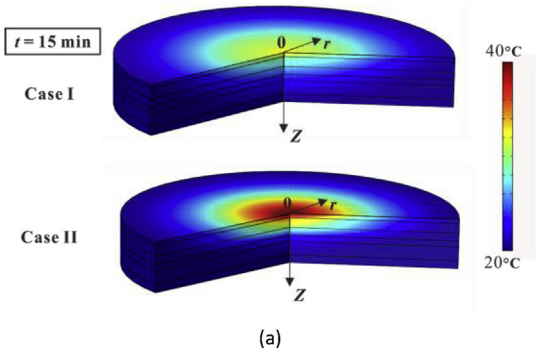

(a)

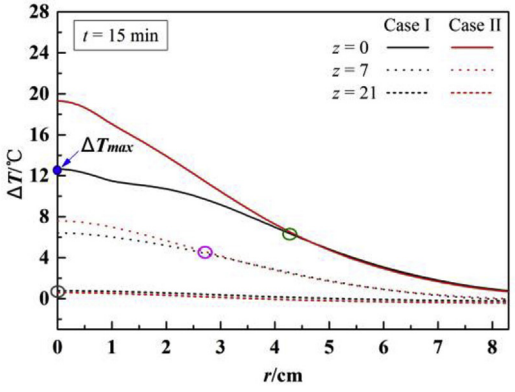

(b)

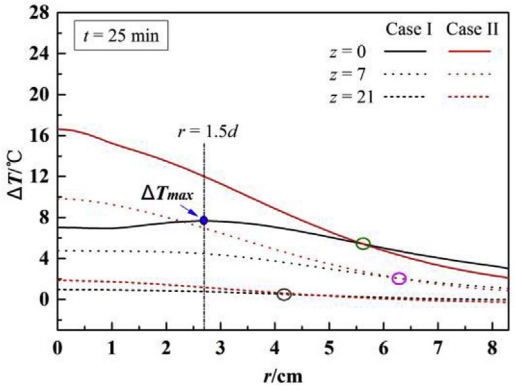

(c)

Fig. 8. Comparison of simulated temperature distribution of in-vitro tissue during moxibusiton without ACDA (Case I) and moxibustion with ACDA (Case II): (a) temperature distribution at t = 15 min. (b) Temperature variation along radius in different depth at t = 15 min (the middle of moxibustion) ; (c) temperature variation along radius in different depth at t = 25 min (the end of moxibustion).

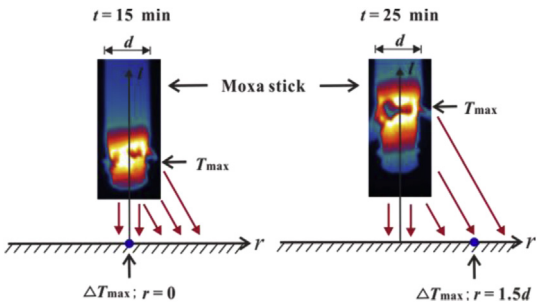

Fig. 9. Schematic diagram of radiation range for burning moxa stick without ACDA at t = 15 min and t = 25 min.

temperature burning area where T_{max} appeared in Fig. 9 moved up gradually. Therefore, the radiation intensity from lower surface of burning moxa stick became weaker with the deposition of ash, and the radiation area of high radiation energy produced by high temperature area moved along r direction with time. These two parts of radiation energy were combinedly absorbed by skin during moxibustion and then were converted into thermal energy leading to temperature rise at skin surface. As a result, the corresponding position of maximum temperature at skin surface moved away from center of treatment site along r direction with time. However, for moxibustion with ACDA, the corresponding position of maximum temperature at skin surface was fixed on the center of treatment site all the time. The reason of this results is that the position of high temperature burning area remained unchanged due to timely ash cleaning on the lower surface of burning moxa stick and distance adjustment. In clinical treatments, the practice of moxibustion is based on the meridian system, and acupoints are distributed along the meridians. The acupoints are believed to be the locations reflecting the disorder of visceral conditions and organs and may have therapeutic effect for certain medical conditions during heat stimulation (Li et al., 2012, 2015) Therefore, the operations of ACDA may improve the efficacy of moxibustion therapy through fixing most of heat stimulation generated by radiation energy from burning moxa stick on the acupoints during the whole moxibustion process.

4.3. Thermal performance of moxibustion in the human abdomen

In clinical moxibustion treatment, ash cleaning and adjustment of treatment distance were performed commonly to keep effective treatment temperature. To better guide the clinical practice, the thermal performance of the human abdomen under moxibustion treatment with different operations were compared experimentally. The moxibustion operations were: moxibustion without ACDA (Case I), moxibustion with ACDA (Case II) and moxibustion with ash cleaning but no distance adjustment (Case III), which were stated in *2.B.* detailedly (as shown in Table 1).

Fig. 10 depicts the surface mean temperatures at abdominal skin surface of five humans under moxibustion treatment. The surface temperature in Case I declined continuously after 2 min of temperature rise due to the ash deposition and upward burning of moxa stick with time. For Case III, the surface temperature curve showed a slight increase and then decreased due to ash deposition among every ash cleaning cycle, but kept one declining trend on the whole due to the rise of treatment distance after a high temperature rise at the beginning. Whereas for Case II, the surface temperature kept fluctuating in the same temperature range approximately from 46 °C to 50 °C among every ash cleaning cycle. Compared Case I and Case III, it can be seen that ash cleaning only was not enough to strength heat stimulation

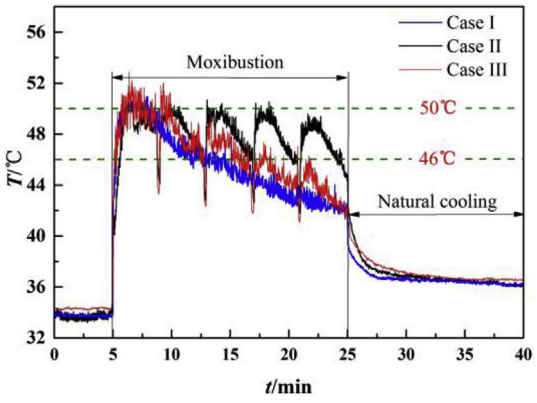

Fig. 10. Surface temperature distribution in human abdominal tissue during moxibustion with three different operations: without ACDA (Case I), with ACDA (Case II) and with ash cleaning but no distance adjustment (Case III).

effectively. While distance adjustment may be reliable to strength heat stimulation by comparing Case II and Case III. However, it was important to note that it was dangerous to perform moxibustion treatment with distance adjustment but no ash cleaning because ash deposition may fall into skin during distance adjustment. Therefore, we compared the thermal performance of human tissue under moxibustion between Case I and Case II detailedly in the next.

According to clinical research (Doherty et al., 2010), different diseases demand different target temperatures ranging from approximately 38 °C–50 °C in thermotherapy treatment. A study by Adriaensen et al. (1983) showed that the temperature at 44.5 °C - 46.5 °C can activate A-fiber mechano-heat-sensitive nociceptors in human skin. And Levine et al. (Levien and Rothschild, 1991) reported that cutaneous M chelonae infection was successfully treated by heating the infected areas to 50 °C. In addition, several researchers have focused on the optimal temperatures of moxibustion for some specific diseases based on the optimal therapeutic effects. For example, a research by Xian et al. (2000) indicated that moxibustion with the skin temperature reaching to 48 °C can inhibit the endotoxin-induced lowing reaction of auricular temperature and have a thermolytic effect on body-fever, while 40 °C had no significant effect. Li et al. (2011) observed that moxibustion above 46 °C activated the subnucleus reticularis dorsalis (SRD) at the rat's medulla oblongata, but below 40 °C or 42 °C, no activation was observed. And in the study of Wang et al. (2013) moxibustion at 46 °C had a significantly greater cholesterol-lowering effect than that at 38 °C. In this study, if 46 °C–50 °C was chosen as the target temperature range of human tissue (Levine and Rothschild, 1991; Li et al., 2011; Wang et al., 2013; Xian et al., 2000), it can be obtained from Fig. 10 that the thermal therapeutic effect on human abdominal tissue may be sustainable and effective during the whole moxibustion process as the surface temperature maintained at 46 °C–50 °C with the operation of ACDA. Relatively, for moxibustion without ACDA, the surface temperature above 46 °C last for only about 6 min as shown in Fig. 10, which may lead to an unsatisfactory efficacy of moxibustion.

The dotted lines in Fig. 11 and Fig. 12 represent simulated predictions of temperature distribution from developed in-vivo moxibustion models for Case I and Case II respectively. The reliability of simulation models was verified by comparing the model predictions of the skin surface temperature with experimental data and a good agreement was obtained, as shown in Figs. 11 and 12. And then the models were used to analyze the effect of ash cleaning on the temperature distributions of human abdominal subcutaneous tissue under moxibustion treatment. It can be found that at the depth of 2 mm and 5 mm, tissue temperature in Case I decreased gradually after a rise at the beginning. While for moxibustion in Case II, tissue temperature at the subcutaneous 2 mm maintained above 46 °C for about 15 min after the temperature increase at the beginning 5 min, so that the moxibustion may take effect at the depth of 2 mm along the whole moxibustion stimulation process. And

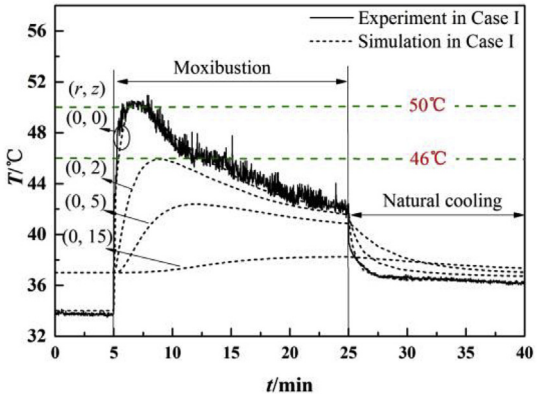

Fig. 11. Temperature distribution in human abdominal tissue during moxibustion without ACDA (Case I) in experiment and simulation.

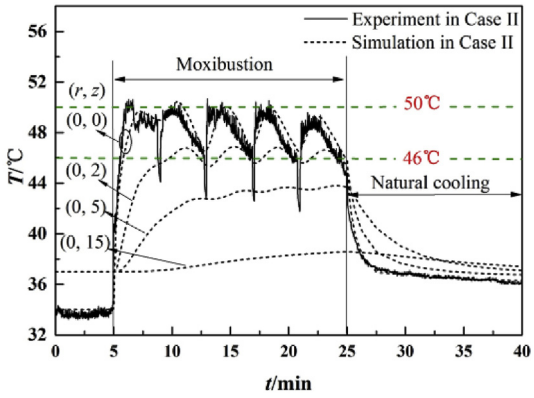

Fig. 12. Temperature distribution in human abdominal tissue during moxibustion with ACDA (Case II) in experiment and simulation.

tissue temperature at subcutaneous 5 mm achieved stabilization after twice of ash cleaning and last for about 10 min. The simulated results indicate that moxibustion with ACDA can extend the duration of high temperature in tissue effectively compared to moxibustion without ash cleaning. Also, it can be implied that deeper tissue (> 5 mm) may be warmed at higher temperature during the moxibustion with ACDA.

5. Conclusions

In this study, a combined experimental and numerical investigation has been conducted on the effect of ACDA on thermal performance of moxibustion therapy. Experiment results show that ash cleaning was an effective way to keep the temperature of moxa stick fluctuating at a high range. And the established models of moxa stick burning with and without ash cleaning showed a good agreement between simulated predictions and experimental results. Based on moxibustion in in-vitro tissue experiment, numerical models of moxibustion with and without ACDA in in-vitro tissue were built. The simulation results indicated that moxibustion with ACDA can produce a lager thermal effect domain in tissue compared to moxibustion without ACDA and the differences between the two thermal effect domains expanded along radius and depth with time. Besides, the corresponding position of maximum temperature at skin surface was fixed on the treatment site during moxibustion with ACDA, which can improve the efficacy of moxibustion therapy. The moxibustion experiment in human abdomen indicated that the thermal therapeutic effect of moxibustion with ACDA may be more sustainable and more effective if 46 °C–50 °C was chosen as the target temperature range of human tissue. In addition, the simulated results of in-vivo moxibustion models indicated that the thermal effect of moxibustion with ACDA can penetrate into subcutaneous tissue (> 2 mm) and lasted a longer time.

Conflicts of interest

The authors have no conflicts of interest or disclosures.

Acknowledgements

This work was supported by the National Natural Science Foundation of China (No.51706177) and the Fundamental Research Funds for the Central Universities.

Appendix A. Supplementary data

Supplementary data to this article can be found online at https://doi.org/10.1016/j.jtherbio.2019.05.018.

References

Adriaensen, H., Gybels, J., Handwerker, H.O., Van Hees, J., 1983. Response properties of thin myelinated (A-delta) fibers in human skin nerves. J. Neurophysiol. 49, 111–122. https://dx.doi.org/10.1152/jn.1983.49.1.111.

Ahuja, A.S., Prasad, K.N., Hendee, W.R., Carson, P.L., 1978. Thermal conductivity and diffusivity of neuroblastoma tumor cells. Med. Phys. 5, 418–421. https://doi.org/10.1118/1.594434.

Chen, R., Lv, Z., Chen, M., An, X., Xie, D., Yi, J., 2011. Neuronal apoptosis and inflammatory reaction in rat models of focal cerebral ischemia following 40-minute suspended moxibustion. Neural Regen. Res. 6, 1180–1184. https://dx.doi.org/10.3969/j.issn.1673-5374.2011.15.011.

Cheng, T.Y., Herman, C., 2011. Optimization of skin cooling for thermographic imaging of near-surface lesions. ASME 2011 International Mechanical Engineering Congress and Exposition. Am. Soc. Mech. Eng. 351–360. 2011. https://dx.doi.org/10.1115/IMECE2011-65221.

Chiu, J.H., 2013. How Does Moxibustion Possibly Work? *Evidence-Based Complementary and Alternative Medicine*. 2013. https://doi.org/10.1155/2013/198584.

Choi, J., Morrissey, M., Bischof, J.C., 2013. Thermal processing of biological tissue at high temperatures: Impact of protein denaturation and water loss on the thermal properties of human and porcine liver in the range 25–80°C. J. Heat Transf. 135, 061302. https://doi.org/10.1115/1.4023570.

Doherty, C.B., Doherty, S.D., Rosen, T., 2010. Thermotherapy in dermatologic infections. J. Am. Acad. Dermatol. 62, 909–927. https://doi.org/10.1016/j.jaad.2009.09.055.

El-Brawany, M.A., Nassiri, D.K., Terhaar, G., Shaw, A., Rivens, I., Lozhken, K., 2009. Measurement of thermal and ultrasonic properties of some biological tissues. J. Med. Eng. Technol. 33, 249–256. https://doi.org/10.1080/03091900802451265.

Erdmann, W.S., Gos, T., 1990. Density of trunk tissues of young and medium age people. J. Biomech. 23, 945–947. https://doi.org/10.1016/0021-9290(90)90360-F.

Henriques Jr., F.C., Moritz, A.R., Moritz, 1947. Studies of thermal injury: I. The conduction of heat to and through skin and the temperatures attained therein. A theoretical and an experimental investigation. Am. J. Pathol. 23, 530–549.

Huang, C., Sheu, T.W.H., 2013. Study of the effect of moxibustion on the blood flow. Int. J. Heat Mass Transf. 63, 141–149. https://doi.org/10.1016/j.ijheatmasstransfer.2013.03.057.

Jeon, B.J., Choi, H.G., 2010. Heat-transfer analysis of indirect moxibustion using unsteady conjugate heat-transfer solutions. J. Mech. Sci. Technol. 24, 2051–2057. https://doi.org/10.1007/s12206-010-0620-0.

Jiang, J., Wang, X., Wu, X., Yu, Z., 2016. Analysis of factors influencing moxibustion efficacy by affecting heat-activated transient receptor potential vanilloid channels. Journal of traditional Chinese medicine = Chung i tsa chih ying wen pan 36, 255–260. https://dx.doi.org/10.1016/S0254-6272(16)30036-X.

Jun, E.M., Chang, S., Kang, D.H., Kim, S., 2007. Effects of acupressure on dysmenorrhea and skin temperature changes in college students: A non-randomized controlled trial. Int. J. Nurs. Stud. 44, 973–981. https://doi.org/10.1016/j.ijnurstu.2006.03.021.

Kim, S.Y., Chae, Y., Lee, S.M., Lee, H., Park, H.J., 2011. The effectiveness of moxibustion: An overview during 10 years. Evid. Based Complement Altern. Med. 2011. https://doi.org/10.1093/ecam/nep163.

Lee, M.S., Kang, J.W., Ernst, E., 2010. Does moxibustion work? An overview of systematic reviews. BMC Res. Notes 3, 284. https://dx.doi.org/10.1186/1756-0500-3-284.

Levine, N., Rothschild, J.G., 1991. Treatment of Mycobacterium chelonae infection with controlled localized heating. J. Am. Acad. Dermatol. 24, 867–870. https://doi.org/10.1016/0190-9622(91)70135-O.

Li, L., Yang, J.S., Rong, P.J., Ben, H., Gao, X.Y., Zhu, B., 2011. Effect of moxibustion-like thermal stimulation with different temperature and covering different areas of" zhongwan"(CV 12) on discharges of neurons in medullary subnucleus reticularis dorsalis of rats. Zhen ci yan jiu = Acupuncture research 36, 313–320.

Li, J., Wang, Q., Liang, H.L., Dong, H.X., Li, Y., Ernest, H.Y.N., Wu, X.K., 2012. Biophysical characteristics of meridians and acupoints: A systematic review. Evid. Based Complement Altern. Med. 2012. https://doi.org/10.1155/2012/793841.

Li, F., He, T., Xu, Q., Lin, L.T., Li, H., Liu, Y., Shi, G.X., Liu, C.Z., 2015. What is the Acupoint? A preliminary review of Acupoints. Pain Med. 16, 1905–1915. https://doi.org/10.1111/pme.12761.

Li, Y., Sun, C., Kuang, J., Ji, C., Feng, S., Wu, J., You, H., 2018. An in vitro and numerical study of moxibustion therapy on biological tissue. IEEE (Inst. Electr. Electron. Eng.) Trans. Biomed. Eng. 65, 779–788. https://dx.doi.org/10.1109/TBME.2017.2719633.

Liu, Q., Sun, T., Liang, H., Bi, D.Y., Liu, H.R., Liu, M., Wu, H.G., Chang, X.R., Liu, M.L., 2017. Clinical observation on the correlation between moxibustion sensation and distance of moxa stick. J. Acupunct. Tuina Sci. 15, 237–241. https://doi.org/10.1007/s11726-017-1007-x.

Myoung, H.S., Lee, K.J., 2014. A unique electrical thermal stimulation system comparable to moxibustion of subcutaneous tissue. Evid. Based Complement Altern. Med. 2014. https://doi.org/10.1155/2014/518313.

Nakamura, S., Nakamura, M., Maeda, E., Nikawa, Y., 2011. Noninvasive temperature measurement during moxibustion using MRI. In: Proc. *APMC*, Melbourne, Australia, 2011, pp. 594–597.

Pennes, H.H., 1948. Analysis of tissue and arterial blood temperatures in the resting human forearm. J. Appl. Physiol. 1, 93–122. https://dx.doi.org/10.1152/jappl.1948.1.2.93.

Petrofsky, J.S., Laymon, M., 2009. Heat transfer to deep tissue: The effect of body fat and heating modality. J. Med. Eng. Technol. 33, 337–348. https://dx.doi.org/10.1080/03091900802069547.

Sakagami, H., Matsumoto, H., Satoh, K., Shioda, S., Ali, C.S., Hashimoto, K., Kikuchi, H., Nishikawa, H., Terakubo, S., Shoji, Y., 2005. Cytotoxicity and radical modulating activity of Moxa smoke. In Vivo 19, 391–397.

Sun, C., Li, Y., Kuang, J., Ji, C., Wu, J., 2017. The effect of ash cleaning cycles on thermal characteristics of moxibustion therapy. ASME 2017 International Mechanical Engineering Congress and Exposition. Am. Soc. Mech. Eng. https://dx.doi.org/10.1115/IMECE2017-71137.

Tang, J.L., Liu, B.Y., Ma, K.W., 2008. Traditional Chinese medicine. Lancet 372, 1938–1940. https://dx.doi.org/10.1016/S0140-6736(08)61354-9.

Torvi, D.A., Dale, J.D., 1994. A finite element model of skin subjected to a flash fire. J. Biomech. Eng. 116, 250–255. https://doi.org/10.1115/1.2895727.

Vardaxis, N.J., Brans, T.A., Boon, M.E., Kreis, R.W., Marres, L.M., 1997. Confocal laser scanning microscopy of porcine skin: Implications for human wound healing studies. J. Anat. 190, 601–611. https://doi.org/10.1046/j.1469-7580.1997.19040601.x.

Wang, L., Xu, B., 2010. Regularity of moxibustion quantity. J. Acupunct. Tuina Sci. 8, 141–144. https://dx.doi.org/10.1007/s11726-010-0392-1.

Wang, G.Y., Wang, L.L., Xu, B., et al., 2013. Effects of moxibustion temperature on blood cholesterol level in a mice model of acute hyperlipidemia: Role of TRPV1. Evid. Based Complement Altern. Med. 2013. https://doi.org/10.1155/2013/871704.

Werner, J., Buse, M., 1988. Temperature profiles with respect to inhomogeneity and geometry of the human body. J. Appl. Physiol. 65, 1110–1118. https://dx.doi.org/10.1152/jappl.1988.65.3.1110.

Wheeler, J., Coppock, B., Chen, C., 2009. Does the burning of moxa (Artemisia vulgaris) in traditional Chinese medicine constitute a health hazard? Acupunct. Med. 27, 16–20. https://doi.org/10.1136/aim.2009.000422.

Wilson, S.B., Spence, V.A., Spence, 1988. A tissue heat transfer model for relating dynamic skin temperature changes to physiological parameters. Phys. Med. Biol. 33, 895–912. https://doi.org/10.1088/0031-9155/33/8/001.

World Health Organization Western Pacific Region, 2007. WHO International Standard Terminologies on Traditional Medicine in the Western Pacific Region, vol. 252. WHO, Geneva, Switzerland, pp. 1–6.

Xia, Y., 2008. Analysis of Heat Transfer and Mathematical Physics Modeling in Moxibustion with Moxa-Stick. Ph.D. dissertation. Dept. Trad. Chin. Med., Guangzhou Univ. of Chinese Medicine, Guangzhou, China.

Xian, M.Q., Dong, Q.S., Zhang, S.H., Dong, S.M., 2000. Thermolytic effect of moxibustion and its relation to acupoint receptors. World J. Acupuncture-Moxibustion 10, 24–31.

Xu, J., Yang, Y., 2009. Traditional Chinese medicine in the Chinese health care system. Health Policy 90, 133–139. https://dx.doi.org/10.1016/j.healthpol.2008.09.003.

Ying, J., Wang, J.P., Yu, X.G., Yin, H.Y., Tang, Y., Qiu, M., Fan, Y.P., Tian, X.N., Zhang, X.W., 2015. Clinical observation of effects on the temperature of Zusanli point by different moxibustion therapies to healthy people. J. Nanjing Univ. Tradit. Chin. Med. 31, 317–319.

Zhou, J.M., Wei, F., Liu, S.J., Zhangm, B.M., 2014. Study on burning temperature versus time graph of moxa sticks in a novel animal moxibustion device. J. Acupunct. Tuina Sci. 12, 194–198. https://dx.doi.org/10.1007/s11726-014-0772-z.